European Journal of Pharmaceutical Sciences 58 (2014) 55–62

Contents lists available at ScienceDirect

European Journal of Pharmaceutical Sciences

journal homepage: www.elsevier.com/locate/ejps

The dynamics of shrinking and expanding drug-loaded microspheres: A semi-empirical approach

Laurent Simon [a,*], Juan Ospina [b], Rebecca Kuntz Willits [c]

[a] Otto H. York Department of Chemical, Biological and Pharmaceutical Engineering, New Jersey Institute of Technology, Newark, NJ 0702, USA
[b] Logic and Computation Group, Physics Engineering Program, School of Sciences and Humanities, EAFIT University, Medellin, Colombia
[c] Department of Biomedical Engineering, The University of Akron, 260 S. Forge St, OLRC 301, Akron, OH 44325-0302, USA

ARTICLE INFO

Article history:
Received 25 January 2014
Received in revised form 7 March 2014
Accepted 19 March 2014
Available online 27 March 2014

Keywords:
Controlled release
Swelling/shrinking microspheres
Hydrogels
Effective time constant
Polymeric drug delivery systems
Analytical solution

ABSTRACT

The dynamics of shrinking and expanding drug-loaded microspheres were studied using a diffusion equation in spherical coordinates. A movable boundary condition was incorporated as a convection term in the original model. The resulting convective-diffusive problem was solved using Laplace transform techniques with the Bromwich integral and the residue theorem. Analytical solutions were derived for the general case of shrinking or expanding microspheres and three particular kinetics expressions: linear growth, exponential swelling and exponential shrinking. Simulations show that microspheres with fast-swelling kinetics released their therapeutic cargo at a relatively slow rate in the first two cases. Ninety-nine percent of the medication was delivered at four times the effective time constant. In line with laboratory studies using bovine serum albumin, an increase in the shrinking rate led to a fast release of the medication from its carrier. The method was applied to analyze insulin transport through spherical Ca-alginate beads. A good agreement was noted between predicted and experimental data. The theoretical effective time constant was 114.0 min.

1. Introduction

As we strive to make better drugs with fewer side effects, regulating and controlling drug delivery has become an increasingly important topic of investigation. Drug delivery from micro- or nano-spheres has the capacity to administer drugs locally, reducing systemic side effects while increasing the dosage delivered to a target site. Hydrogels, or other swellable polymeric systems, are widely studied as potential mucoadhesives or drug-delivery vehicles. However, many of these novel materials that would serve to encapsulate drugs have significant changes in size. Structural alterations occur during the release of medication which complicates the analysis of hydrogel-based delivery devices and the prediction of their performance. As a result, a feasibility study, to assess whether these products are suitable for a particular application, tends to proceed without the assistance of computer simulations.

Drugs released from scaffolds is generally diffusion- and/or erosion-controlled. Degradable materials, particularly polyesters, are popular materials for microparticle-based drug delivery. The transport of molecules through these microspheres is, typically, controlled by the degradation of the material and the diffusion of drug that happens during this process (see Panyam and Labhasetwar, 2003 for more details). Drug-loaded hydrogel microspheres have been utilized for over 20 years as potential gastroenteric delivery vehicles, primarily by the oral route (Neeraj et al., 2011). The pH of the environment makes many hydrogels mucoadhesive which leads to the binding of the mucosa while delivering active agents. The swelling triggers drug release and accompanied by a polymer chain relaxation. Both of these processes (e.g., binding and swelling) may contribute to the release kinetics. In addition, the molecular structure of the hydrogel and the chemistry of the environment can alter the drug-delivery profile. These various mechanisms require additional modeling tools to fully understand the delivery rates.

Particularly in hydrogels, the drug may be diffused out of the device at a faster rate than any erosion that would occur. For example, chitosan-based microspheres developed to encapsulate anastrozole, a breast cancer treatment, had ~80% release in 12 h and only ~3% erosion (Shavi et al., 2011). However, surface degradation is only one mechanism that serves to alter the size of these microspheres. Size changes due to swelling can be significant, particularly in triggered-release systems. Chitosan-poly(ethylene oxide) microspheres have been developed to swell in acidic environments, such as the stomach, and can be used to deliver drugs for stomach cancer (Patel Vijay and Amiji Mansoor, 1996).

* Corresponding author. Tel.: +1 9735965263.
E-mail address: laurent.simon@njit.edu (L. Simon).

http://dx.doi.org/10.1016/j.ejps.2014.03.005
0928-0987/

In addition, hydrogels have been designed to swell or de-swell, based on the pH shift that occurs during the oxidation of glucose (Klumb and Horbett, 1992; Kost et al., 1985) for the manufacturing of insulin-delivery systems.

Several stimuli (e.g., temperature, pH) have been applied to increase the swelling of hydrogels (Gupta et al., 2002). The pH-responsive materials are made of polymeric backbones with the attachment of ionic groups, such as acrylamide and methacrylic acid. Anionic hydrogels swell when the pendant groups are un-ionized below or ionized above the pK_a of the polymeric network. This behavior is due to the large osmotic pressure induced by the presence of ions (Gupta et al., 2002). The swelling and shrinking of environment-sensitive hydrogels have also been explored as a way of modulating drug delivery (Qiu and Park, 2001). At low pH, hydrogels made of poly(methacrylic acid) (PMA) and poly(ethylene glycol) (PEG) shrink because of interactions between the acidic protons of the carboxyl groups of PMA and the ether oxygen of PEG. The ionization of the carboxylic groups of PMA at high pH leads to swelling (Qiu and Park, 2001).

Because of the potentials of these hydrogels to be used to control drug-release kinetics, mathematical models have been developed to predict their behaviors. Analysis of the transport characteristics of swollen polymers is usually conducted using diffusional Deborah (*De*) and swelling interface (*Sw*) numbers (Brazel and Peppas, 1999). The former parameter measures the solvent motion relative to the relaxation of the polymer; *Sw* connects solvent motion, or penetrant uptake, to the solute release by diffusion. Power-law type models are applied to estimate the diffusion coefficient or determine the relative contributions of Fickian diffusion and relaxation. In spite of their popularity, these equations do not incorporate the swelling and shrinking kinetics of the gel, which makes it difficult to simulate the effects of the rate and degree of swelling on drug transport through a polymeric network. In addition, the influence of the swelling patterns on the time elapsed before releasing the active ingredient can only be determined experimentally in the current framework. Note that the power-law models only provide early-time estimations of the release dynamics (Torres-Lugo and Peppas, 1999).

This contribution focuses on release kinetics of drug-loaded microspheres. The delivery system is allowed to shrink or swell during administration of the medicine. A mathematical model which includes the effects of convection is presented in the first section. The transport problem is solved and a procedure to estimate the system's effective time constant is outlined. The second section considers different kinetics of swelling and shrinking of the microspheres. Examples are provided in Section 3.

2. Materials and methods

2.1. Mathematical modeling

Using vector notation, the general model of transport though a microsphere involves the effects of diffusion and convection:

$$\frac{\partial c}{\partial t} = \nabla \cdot (D \nabla c) - \nabla \cdot (c\mathbf{u}) \tag{1}$$

where c is the drug concentration, D is its diffusion coefficient through the material, $\mathbf{u}$ is the fluid velocity and t is the time. The drug is initially entrapped in a glassy polymer (Fig. 1). Its concentration is uniform throughout the domain $0 < r < R_1$ at the beginning of the experiment. Upon contact with the fluid, the polymer expands outward to the position $R(t)$. The directions of drug diffusion and fluid transport are shown in Fig. 1.

Eq. (1) explains drug release from swollen microspheres where transport is facilitated mainly by diffusion. In this case, the solvent flows in a direction opposite to that of the drug molecules. For a de-swelling microsphere, its volume is reduced as the fluid is expelled from the microsphere. This time, convection is in the same direction as diffusion. Consequently, drug transport is promoted by the convective flow. Assuming a constant D, Eq. (1) becomes

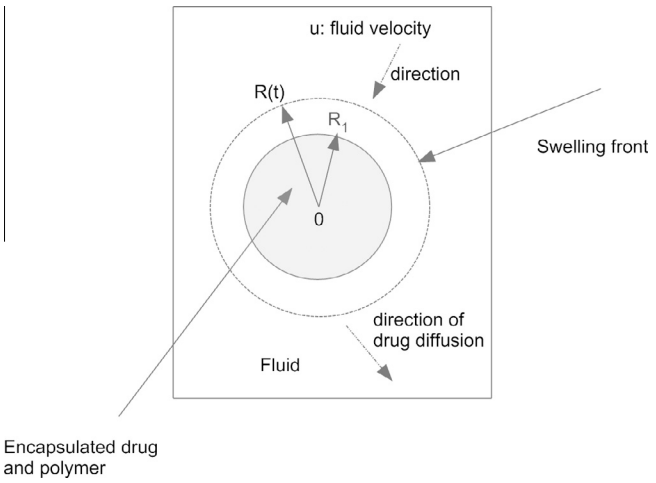

Fig. 1. The drug encapsulated in a polymer is surrounded by a fluid. At the beginning of the experiment, the polymer is a glassy state in the region $0 < r < R_1$. Upon contact with the fluid, the domain extends to $R(t)$.

$$\frac{\partial c}{\partial t} = D\nabla^2 c - \nabla \cdot (c\mathbf{u}) \tag{2}$$

Eq. (2) is written in spherical coordinates as:

$$\frac{\partial c}{\partial t} = D\frac{1}{r^2}\frac{\partial}{\partial r}\left(r^2\frac{\partial c}{\partial r}\right) - \frac{1}{r^2}\frac{\partial}{\partial r}(r^2 cu) \tag{3}$$

for a one-dimensional transport along the radial direction, i.e., $\mathbf{u} = u\mathbf{e_r}$; r is the radial variable. One of the main assumptions in the model is that no inert structure is present in the microspheres. The Cartesian form of Eq. (1) was used in previous investigations of transport through swellable materials (Brazel and Peppas, 1999).

Because of the presence of a velocity gradient across the boundary $[0, R(t)]$, the following equation holds (Bierbrauer, 2005):

$$u(R(t), t) - u(0, t) = \int_0^{R(t)} \frac{\partial u}{\partial r} dr \tag{4}$$

which can be written in terms of a change in the boundary as:

$$\frac{dR}{dt} = \int_0^{R(t)} \frac{\partial u}{\partial r} dr \tag{5}$$

where $R(t)$ is the radius of the growing domain. If we assume uniform growth, i.e. $\partial u/\partial r$ is only a function of time, the following two equations are derived:

$$\frac{\partial u}{\partial r} = \frac{1}{R}\frac{dR}{dt} \tag{6}$$

and

$$u(r, t) = \frac{1}{R}\frac{dR}{dt} r \tag{7}$$

The justification for writing $\partial u/\partial r$ as a function of time alone is given in the appendix. This assumption is valid for spherical flow with constant density (ρ) and viscosity (μ). In the case of swelling, the fluid density is expected to change with t and in the r-direction. The approach adopted in this work is appropriate for the motion of a Newtonian fluid with a constant velocity and a slightly changing density such that $D\rho/Dt \approx 0$. A steady-state velocity profile is established quickly.

Eq. (3) becomes

$$\frac{\partial c}{\partial t} = D\frac{1}{r^2}\frac{\partial}{\partial r}\left(r^2\frac{\partial c}{\partial r}\right) - \left(\frac{\dot{R}}{R}r\right)\frac{dc}{dr} - 3\frac{\dot{R}}{R}c \tag{8}$$

after substituting Eqs. (6) and (7) in Eq. (3) where $\dot{R} = dR/dt$. In this framework, drug release is governed by diffusion and the velocity of the water front moving through the polymeric matrix (Fig. 1). As the solvent penetrates the polymer, the glass transition temperature is lowered. The polymer then swells and two distinct regions, consisting of a glassy and rubbery state, are observed. The interface between these two domains moves towards the center of the sphere (i.e. R_1). Molecular diffusion through the glassy region is negligible. A moving boundary condition is usually applied to describe transport across the rubbery state.

Initially, the drug concentration in the sphere is

$$c(r,0) = 1 \tag{9}$$

The boundary conditions are

$$R(0) = R_1 \tag{10}$$

$$\frac{\partial c(0,t)}{\partial r} = 0 \tag{11}$$

where R_1 is the initial radius of the sphere. A dimensionless concentration is used in Eqs. (8), (9), and (11). The solution can be easily generalized for a loading dose of c_0. A symmetry condition is applied at the center of the microsphere (i.e., Eq. (11)). The perfect sink approximation at $R(t)$ implies that

$$c(R(t),t) = 0 \tag{12}$$

The following change of variable is performed

$$r = \zeta R(\tau) \tag{13}$$

to remove the time-dependent boundary condition. The goal of replacing the variable r with $\zeta R(\tau)$ is to reduce the problem to one with a constant boundary condition that is easier to solve. As a result, Eq. (8) becomes

$$\frac{\partial c(\zeta,\tau)}{\partial \tau} = D\left[\frac{2\frac{\partial c(\zeta,\tau)}{\partial \zeta} + \zeta\frac{\partial^2 c(\zeta,\tau)}{\partial \zeta^2}}{\zeta R(\tau)}\right] - 3\frac{\frac{dR(\tau)}{d\tau}c(\zeta,\tau)}{R(\tau)} \tag{14}$$

Further, it is desirable to find a form of Eq. (14) that does not include $dR(\tau)/d\tau$. With the following transformation:

$$c(\zeta,\tau) = \frac{C(\zeta,\tau)}{R(\tau)^3} \tag{15}$$

Eq. (14) becomes

$$R(\tau)^2\frac{\partial C(\zeta,\tau)}{\partial \tau} = D\left[\frac{2}{\zeta}\frac{\partial C(\zeta,\tau)}{\partial \zeta} + \frac{\partial^2 C(\zeta,\tau)}{\partial \zeta^2}\right] \tag{16}$$

The variable C is defined as R^3c. Before applying the Laplace operator, Eq. (16) is written as

$$\frac{\partial C(\zeta,\sigma)}{\partial \sigma} = D\left[\frac{2}{\zeta}\frac{\partial C(\zeta,\sigma)}{\partial \zeta} + \frac{\partial^2 C(\zeta,\sigma)}{\partial \zeta^2}\right] \tag{17}$$

where

$$\sigma = \int_0^\tau \frac{1}{R(\chi)^2}d\chi \tag{18}$$

The new initial and boundary conditions are

$$C(\zeta,0) = R(0)^3 \tag{19}$$

and

$$\frac{\partial C(0,\sigma)}{\partial \zeta} = 0 \tag{20}$$

$$C(1,\sigma) = 0 \tag{21}$$

respectively.

Techniques, such as the separation of variables and Laplace transforms, can be used to solve the system formed by Eqs. (17), (19), (20), (21). The latter method involves the application of the Laplace operator to both sides of Eq. (17) to yield an ordinary differential equation:

$$s\overline{C}(\zeta,s) - C(\zeta,0) = D\left[\frac{2}{\zeta}\frac{d\overline{C}(\zeta,s)}{d\zeta} + \frac{d^2\overline{C}(\zeta,s)}{d\zeta^2}\right] \tag{22}$$

with the transformed boundary conditions:

$$\frac{dC(0,s)}{d\zeta} = 0 \tag{23}$$

and

$$\overline{C}(1,s) = 0 \tag{24}$$

where $\overline{C}(\zeta,s)$ is the Laplace transform of $C(\zeta,\sigma)$, defined by $\overline{C}(\zeta,s) = \int_0^\infty e^{-s\sigma}C(\zeta,\sigma)d\sigma$. The method of Laplace transform is a useful tool for solving linear ordinary (ODEs) and partial differential equations (PDEs). In the latter case, the PDE is reduced to an ODE and the boundary conditions are transformed using the Laplace operator. The solution to the resulting problem is obtained after applying techniques suitable for solving ODEs. The final step involves the use of inverse Laplace transforms to yield the solution of the original PDE in the time domain.

The solution of Eq. (22), after considering Eqs. (19), (23), and (24), is

$$\overline{C}(\zeta,s) = R(0)^3\left[-\frac{\sinh\left(\zeta\sqrt{\frac{s}{D}}\right) - \zeta\sin h\left(\sqrt{\frac{s}{D}}\right)}{s\zeta\sin h\left(\sqrt{\frac{s}{D}}\right)}\right] \tag{25}$$

An analytical solution can be derived for the concentration profile by applying the residue theorem:

$$C(\zeta,\sigma) = \sum_{n=1}^{\infty}\frac{P(s_n)}{\left.\frac{dQ(s)}{ds}\right|_{s=s_n}}e^{s_n\sigma} \tag{26}$$

with $P(s)$ defined as the numerator of $\overline{C}(\zeta,s)$,

$$P(s) = R(0)^3\left[-\sinh\left(\zeta\sqrt{\frac{s}{D}}\right) + \zeta\sinh\left(\sqrt{\frac{s}{D}}\right)\right] \tag{27}$$

and

$$Q(s) = s\zeta\sinh\left(\sqrt{\frac{s}{D}}\right) \tag{28}$$

Eq. (26) is used in this contribution because the inverse Laplace transform of the function in Eq. (25) is not readily available from tables of Laplace transform. The poles, defined as $s_0 = 0$ and $s_n = -n^2\pi^2D$ for $n = 1 \ldots \infty$, are the values of s when $Q(s) = 0$. Note that the steady-state concentration is $\lim_{s\to 0} s\overline{C}(\zeta,s) = 0$. Eq. (26) can be manipulated to yield

$$C(\zeta,\sigma) = 2R(0)^3\sum_{n=1}^{\infty}\left(-\frac{\sin(n\pi\zeta)e^{-n^2\pi^2D\sigma}}{\zeta(-1)^n n\pi}\right) \tag{29}$$

or

$$c(r,t) = \frac{2R(0)^3}{R(t)^2}\sum_{n=1}^{\infty}\left(-\frac{\sin(\frac{n\pi r}{R(t)})\exp\left(-n^2\pi^2D\int_0^t\frac{1}{R(\chi)^2}d\chi\right)}{r(-1)^n n\pi}\right) \tag{30}$$

in terms of the original variables.

The percentage of drug released from the sphere is defined as

$$M(t) = 1 - \frac{\int_0^{R(t)} r^2 c(r,t) dr}{\int_0^{R(0)} r^2 c(r,0) dr} \tag{31}$$

Substitution of Eq. (30) in (31) gives:

$$M(t) = 1 - \frac{6}{\pi^2} \sum_{n=1}^{\infty} \left[\frac{1}{n^2} \exp\left(-n^2 \pi^2 D \int_0^t \frac{1}{R(\chi)^2} d\chi \right) \right] \tag{32}$$

The effective time constant is defined by Collins, 1980:

$$t_{eff} = \int_0^{\infty} t\Omega(t) dt \tag{33}$$

where $\Omega(t)$ stands for the probability density function:

$$\Omega(t) = \frac{(g_e - g(t))}{\int_0^{\infty} (g_e - g(t)) dt} \tag{34}$$

Eq. (33) can be written using the Laplace variable s:

$$t_{eff} = \lim_{s \to 0} \left(\frac{\psi_{ss}}{s^2} + \frac{d\bar{\psi}(s)}{ds} \right) \left[\lim_{s \to 0} \left(\frac{\psi_{ss}}{s} - \bar{\psi}(s) \right) \right]^{-1} \tag{35}$$

where ψ_{ss} is the equilibrium value and $\bar{\psi}$ is the Laplace transform of ψ (i.e., $M(t)$).

2.2. Kinetics of swelling and shrinking of microspheres

Several models exist to describe the swelling or shrinking of delivery systems (Schott, 1992; Zrinyi et al., 1993). Pirvu applied a Korsmeyer-based equation to study the release of xantinol nicotinate from gelatin microspheres (Pirvu, 2004). Martinez-Ruvalcaba et al., 2009, used a second-order equation to investigate the swelling behavior of polyacrylamide-co-itaconic acid/chitosan hydrogels. The swelling capacity of the gel decreases with an increase in the chitosan concentration. This decrease in swelling leads to a reduction in the value of the diffusion coefficient of ascorbic acid. Three kinetic patterns are addressed in this study as they represent a wide range of experimental observations.

2.2.1. Case I. Linear growth

In the case of a linear growth, the boundary layer takes the following form:

$$R(t) = \begin{cases} R_1(1 + \alpha t) & \text{if } t < \frac{R_2 - R_1}{\alpha R_1} \\ R_2 & \text{if } t \geqslant \frac{R_2 - R_1}{\alpha R_1} \end{cases} \tag{36}$$

The percentage of drug released is given by Eq. (32) with $R(\chi)$ defined by Eq. (36). According to Eq. (36), a microsphere of radius R_1 increases linearly to an equilibrium size of R_2. It takes $(R_2 - R_1)/\alpha R_1$ unit time for the microsphere to reach R_2. No further change is observed in the dimension of the carrier. In investigating the suitability of novel interpenetrating network hydrogels as carriers for oral drug delivery, researchers noticed a linear swelling profile when the pH was suddenly changed from 2 to 7.4 (Chivukula et al., 2006).

2.2.2. Case II. Exponential growth

Some hydrogels show exponential growth when immersed in aqueous solvents. The size of polyacrylamide hydrogels increases exponentially when placed in low concentration NaCl solutions (Sivanantham and Tata, 2012). Studies conducted by Tabaka also indicate similar behavior during swelling (Tanaka, 1979). The boundary layer takes the empirical form:

$$R(t) = R_{10}(1 - be^{-\alpha t}) \tag{37}$$

where the initial length from Eq. (10) is $R(0) = R_1 = R_{10}(1 - b)$. Thus, the fraction of the initial dose that is released becomes

$$M(t) = 1 - \frac{6}{\pi^2} \sum_{n=1}^{\infty} \left[\frac{1}{n^2} \exp\left(-\frac{\pi^2 D n^2 \left(b\left(\frac{1}{b - e^{\alpha t}} + \frac{1}{1-b}\right) + \log(e^{\alpha t} - b) - \log(1-b) \right)}{\alpha R_1^2} \right) \right] \tag{38}$$

2.2.3. Case III. Exponential shrinking

In some experiments, hydrogels shrink when transferred from NaCl solution to deionized water (Sivanantham and Tata, 2012). For a shrinking sphere, the radius changes as a function of time according to the following equation:

$$R(t) = R_1 e^{-\alpha t} \tag{39}$$

The closed-form expression $M(t)$ is

$$M(t) = 1 - \frac{6}{\pi^2} \sum_{n=1}^{\infty} \left[\frac{1}{n^2} \exp\left(-\frac{\pi^2 D n^2 (e^{2\alpha t} - 1)}{2\alpha R_1^2} \right) \right] \tag{40}$$

3. Results and discussion

3.1. Drug- release simulations

The following parameters were chosen to study the effects of linear growth kinetics on the drug release pattern: $R_0 = 1$, $R_{01} = 1.5$ and $D = 0.1$ (Fig. 2). As α increased from 0.2 to 0.4, the fraction of drug released from the sphere decreased. The swelling kinetics is shown in Fig. 2b. A hydrogel with fast swelling kinetics will release the drug at a relatively slow rate. In practice, this condition, which results from a rapid diffusion of water through the network, is

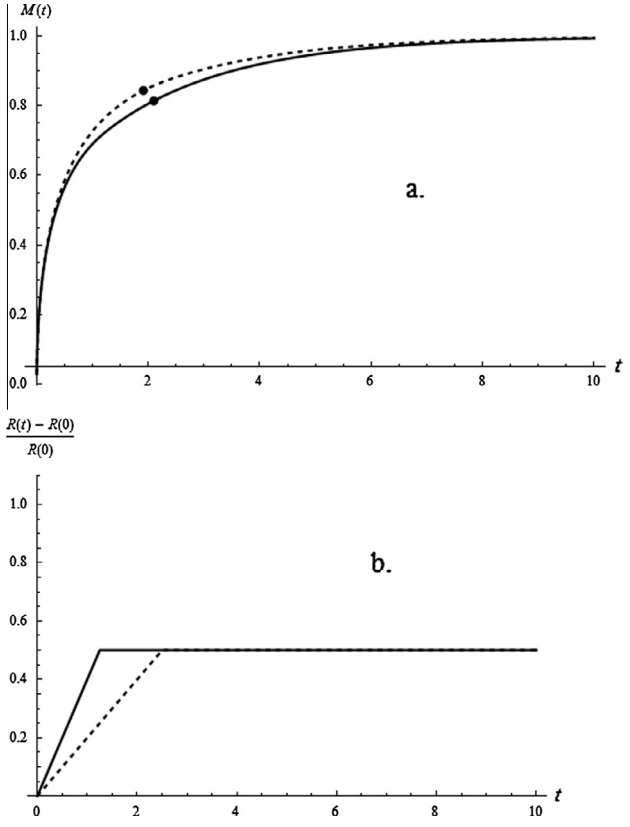

Fig. 2. Percentage of drug released as a function of the linear growth rate (panel a). The following model was applied: $R(t) = R_0(1 + \alpha t)$ if $t < \frac{R_{01} - R_0}{\alpha R_0}$ or $R(t) = R_{01}$ if $t \geqslant \frac{R_{01} - R_0}{\alpha R_0}$ with $R_0 = 1$, $R_{01} = 1.5$ and $D = 0.1$. Plots were generated for $\alpha = 0.2$ (- - -) and $\alpha = 0.4$ (—). The swelling ratio is displayed in panel b.

achieved by preparing small particles of dried hydrogels or fabricating porous hydrogels (Mahmoud et al., 2010). The quick-swelling property of polymers makes them ideal for creating gastric retention devices, which produce long-term, oral drug delivery (Chen et al., 2000). The effective time constant of the process is an important design parameter that can be considered in selecting components, such as monomers and cross linkers, that influence the release behavior. Based on the data used in the simulation, the following constants were calculated after using Eq. (33): $t_{eff}(0.2) = 1.92$ and $t_{eff}(0.4) = 2.10$ (Fig. 1a). If $M(t)$ is approximated as a first-order process, $t_{eff}(\alpha)$ represents the time constant of the system for a particular α (Simon, 2013). The response time, defined as the period elapsed to reach 98% of the steady-state value, is equal to $4t_{eff}(\alpha)$. Application of Eq. (32) yields 0.99 for $4t_{eff}(0.2)$ and $4t_{eff}(0.4)$. As α is determined by the mechanical properties of the hydrogel, its value can be adjusted to reach a desired t_{eff}.

The fraction of drug released as a function of the exponential growth rate α is shown in Fig. 3. Using Eq. (37), the following parameters were set for the simulation: $R_{10} = 1$, $b = 0.5$ and $D = 0.01$. The parameter α was allowed to vary from 0.2 to 0.4. As noticed in the linear case, the percentage of drug released is reduced with a surge in α (Fig. 3a). The effective time constants are $t_{eff}(0.2) = 8.16$ and $t_{eff}(0.4) = 9.21$. Ninety-nine percent of the medication is delivered at $4t_{eff}(0.2)$ and $4t_{eff}(0.4)$. In cases of linear and exponential growths, the increase in the diffusional path travelled by the solute, due to swelling, led to a decrease in the drug release rate. This hypothesis may help explain the $M(t)$ behavior at constant α (Figs. 2 and 3). When α changes from 0.2 to 0.4, $M(t)$ is expected to decline because the expansion in the size of the boundary layer (i.e., path available for diffusion) occurs at a faster rate (Fig. 3b).

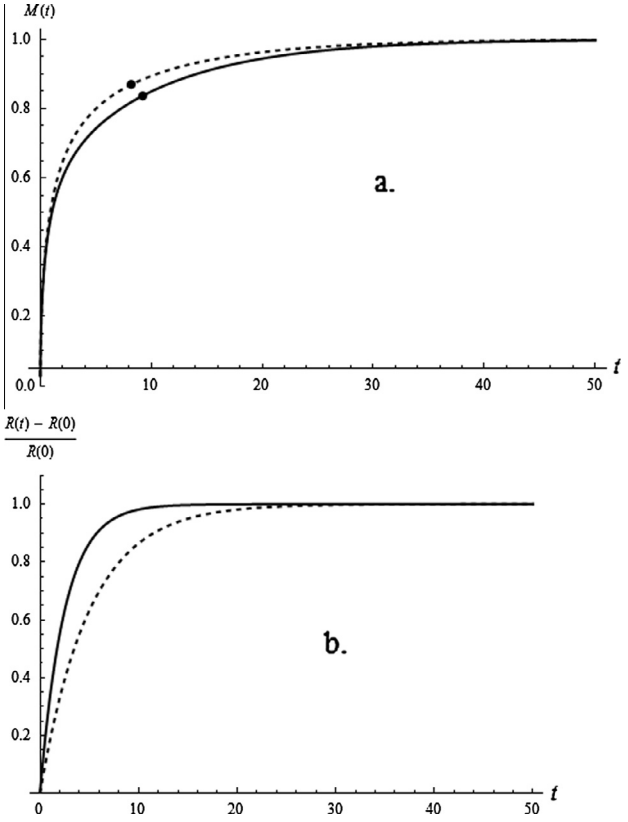

Fig. 3. Percentage of drug released as a function of the exponential growth rate (panel a). The following equation was applied: $R(t) = R_{10}(1 - be^{-\alpha t})$ with $R_{10} = 1$, $b = 0.5$ and $D = 0.01$. Plots were generated for $\alpha = 0.2$ (- - -) and $\alpha = 0.4$ (—). The swelling ratio is displayed in panel b.

As the shrinking rate increases from $\alpha = 0.2$ to $\alpha = 0.4$ (Eq. (39)), the drug is released from the carrier (Fig. 4) at a faster rate. The model parameters used are $R_1 = 1$ and $D = 0.1$. In this simulation, the effective time constants calculated are: $t_{eff}(0.2) = 0.59$ and $t_{eff}(0.4) = 0.46$. Ninety-nine percent of the drug is released at $4t_{eff}(0.2)$ and $4t_{eff}(0.4)$ (Fig. 4a). The de-swelling kinetics is shown in Fig. 4b. These results are consistent with published findings. Studying the behavior of bovine serum albumin (BSA) release from poly(N-isopropylacrylamide) hydrogels, Naddaf et al., 2010, were able to vary the shrinking kinetics by conducting experiments at

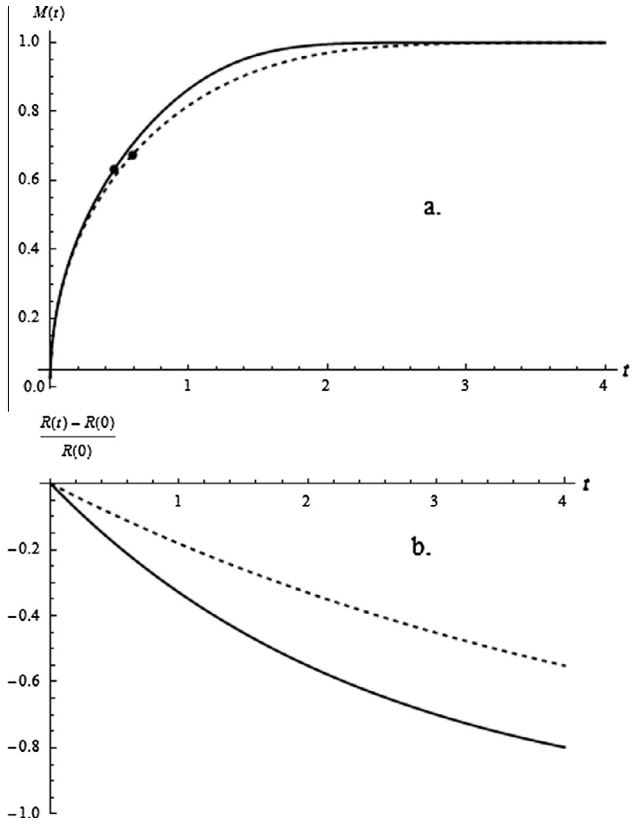

Fig. 4. Percentage of drug released as a function of the shrinking rate (panel a). The following model was applied: $R(t) = R_1 e^{-\alpha t}$ with $R_1 = 1$ and $D = 0.1$. Plots were generated for $\alpha = 0.2$ (- - -) and $\alpha = 0.4$ (—). The shrinking ratio is displayed in panel b.

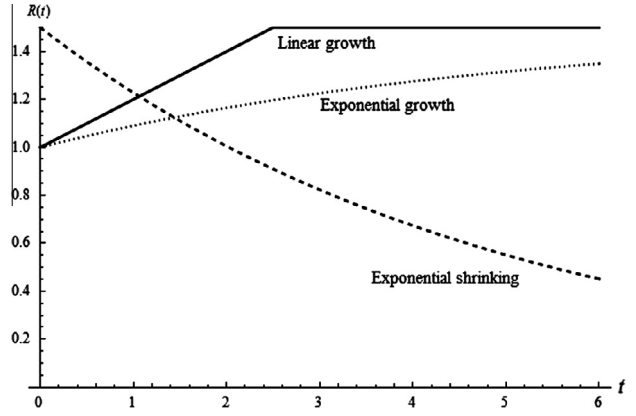

Fig. 5. Swelling/de-swelling kinetics. Shrinking of the microsphere was described by $R(t) = 1.5e^{-0.2t}$. The exponential growth was given by $R(t) = 1.5(1 - 0.33e^{-0.2t})$. For the linear growth, $R(t) = 1.0(1 + 0.2t)$ if $t < (R_{01} - R_0)/\alpha R_0 = 2.5$ and $R(t) = 1.5$ if $t \geqslant 2.5$.

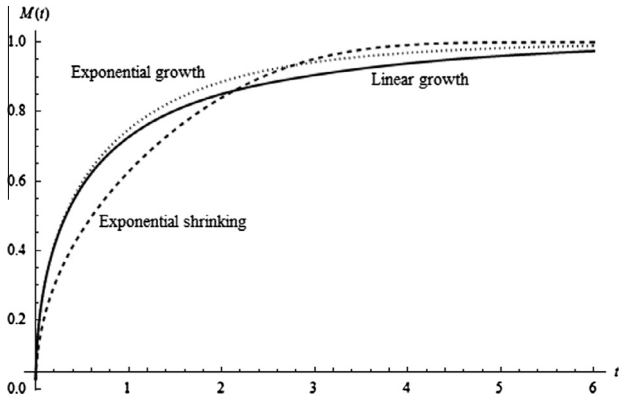

Fig. 6. Percentage of drug released as a function of the type of swelling/de-swelling kinetics. For the simulations, the swelling behaviors in Fig. 4 were used; the diffusion was set to 0.1.

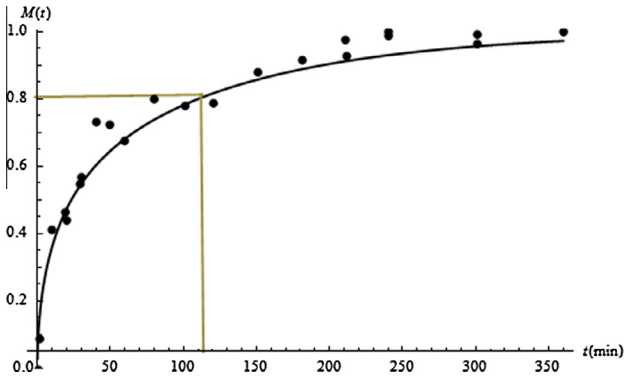

Fig. 7. Predicted percentage of insulin released (–). The following model was applied: $R(t) = R_{10}(1 - be^{-\alpha t})$ with $R_{10} = 1.62$ mm, $b = 0.27$, $\alpha = 0.019$ min^{-1} and $D = 0.0021$ mm^2/min. The experimental data (•) are obtained from Fig. 6 in the work by Rasmussen et al. (2003). The effective time constant is 114.0 min.

different temperatures. By increasing the shrinking rate of the hydrogel, the BSA was released at a faster rate.

Figs. 5 and 6 show the effects of the type of swelling/de-swelling on the release kinetics. The following model was used to describe shrinking of the microsphere: $R(t) = 1.5e^{-0.2t}$. Exponential growth was described by $R(t) = 1.5(1-0.33e^{-0.2t})$ so that the initial and final radii were 1.0 and 1.5, respectively. These specifications matched the linear growth profile where $R(t) = 1.0(1 + 0.2t)$ if $t < (R_{01} - R_0)/\alpha R_0 = 2.5$ and $R(t) = 1.5$ if $t \geqslant 2.5$ (Fig. 5). For the simulations, D was set to 0.1. At the beginning of the experiment, more drug was released from the exponentially swollen gel compared to the other systems (Fig. 6). This behavior can be explained in terms of the path available for solute diffusion, as discussed earlier. The de-swelling gel ultimately led to a faster release as the diffusional distance was reduced. Drug transport was also enhanced by fluid convection during shrinking.

3.2. Experimental release data

In the previous examples, simulations were performed using sets of dimensionless parameter values. In practice, the model parameters need to be estimated from laboratory data. Certain variables, such as the size of the microsphere should also be available throughout the experiments. To show the application of the method outlined above, insulin release data were obtained from swelling spherical Ca-alginate beads (Rasmussen et al., 2003). The insulin was in the form of hexamer, Mw 39 kD. Procedures for preparing the protein-loaded beads were given (Rasmussen et al., 2003). In summary, droplets of an insulin–alginate solution were pipetted into an insulin–$CaCl_2$ solution. The latter mixture was obtained by dissolving 375 mg of dry insulin in 250 ml 2% (w/v) $CaCl_2$. For the diffusion experiments, beads were transferred to a 10-ml artificial spinal fluid (ACSF) buffer contained in a test tube which was then placed on a blood shaker rotating at 20 rpm. The swelling of the beads was determined gravimetrically and the insulin concentration was measured by the method of Bradford (Bradford, 1976). A numerical solution strategy was adopted to solve a model similar to Eq. (1) (Rasmussen et al., 2003). The prediction agreed very well with experimental data and confirmed the inclusion a convection term to explain the transport mechanism.

Data for the average radius of the alginate bead were first read from Fig. 5 in the published article (Rasmussen et al., 2003) using a digitizing software, Engauge Digitizer (Mitchell, 2007). Eq. (37) was fit to the bead radius yielding the following parameter values: $R_{10} = 1.62$ mm, $b = 0.27$ and $\alpha = 0.019$ min^{-1}. The listed diffusion coefficient (Rasmussen et al., 2003) was substituted in Eq. (38) to calculate a predicted fraction of insulin released profile: $D = 0.0021$ mm^2/min. Fig. 7 shows that the experimental and predicted $M(t)$ agree very well at small time. A small deviation is noticed at larger time, which may be due to the approximated D value. The effective time constant was 114.0 min and 98.7% of the insulin was released at the calculated $4t_{eff}$. These findings show that the method is applicable to the modeling of insulin release from swelling Ca-alginate beads.

4. Conclusion

The transient release behaviors of swelling and shrinking of drug-loaded microspheres were modeled using an advection–diffusion equation in spherical coordinates. One of the boundaries was assumed to move at a uniform velocity while the other, located at the center, remained stationary. An analytical expression for the fraction of drug released was derived after removing the time-dependent boundary condition and applying Laplace transform techniques. A procedure for calculating the effective time constant of the system was outlined. Three behaviors, namely linear growth, exponential swelling and de-swelling kinetics, which have been observed in hydrogels, were simulated to illustrate the methodology. As the slope of the linear growth model increased, the fraction of drug released from the gel at a particular time decreased. The time constant was higher for a larger slope. Similar observations were made when the exponential growth rate of hydrogels changed from 0.2 to 0.4. The decline in the drug release rate may be explained by the stretching of the diffusional path of the drug molecules. Contrary to those findings, drug molecules were released from the carrier at a faster rate as the shrinking rate of hydrogels increased. Ninety-nine percent of the medication was delivered at four times the effective time constant. This number may serve as a design criterion and help in the selection of components, such as monomers and cross linkers. The methodology was applied, successfully, to a study describing the release of insulin from spherical Ca-alginate beads.

Appendix A

A.1. Determination of the fluid velocity profile

The Navier–Stokes equation applied to the fluid in a sphere is:

$$\rho\frac{\partial u(r,t)}{\partial t} + \rho u(r,t)\frac{\partial u(r,t)}{\partial r} = -\frac{\partial P(r,\theta,\phi)}{\partial r} - \frac{2\mu u(r,t)}{r^2} + \mu\frac{\partial^2 u(r,t)}{\partial r^2} + 2\mu\frac{1}{r}\frac{\partial u(r,t)}{\partial r} \qquad (1A)$$

where ρ and μ are the density and viscosity of the fluid. For a negligible change in the pressure P in the r-direction, we have:

$$\rho\frac{\partial u(r,t)}{\partial t}+\rho u(r,t)\frac{\partial u(r,t)}{\partial r}=-\frac{2\mu u(r,t)}{r^2}+\mu\frac{\partial^2 u(r,t)}{\partial r^2}+2\mu\frac{1}{r}\frac{\partial u(r,t)}{\partial r} \tag{2A}$$

or

$$\rho\frac{\partial u(r,t)}{\partial t}=-\frac{2\mu u(r,t)}{r^2}+\mu\frac{\partial^2 u(r,t)}{\partial r^2}+2\mu\frac{1}{r}\frac{\partial u(r,t)}{\partial r} \tag{3A}$$

at low Reynolds number. The initial and boundary conditions are

$$u(r,0)=0 \tag{4A}$$

and

$$u(R,t)=V \tag{5A}$$

respectively, where V is the fluid velocity as the solvent moves in (expansion) or out (contraction) of the sphere. Note that V is positive in the case of swelling and negative when the sphere shrinks.

To solve the system formed by Eqs. (3A), (4A), and (5A), the Laplace transform of Eq. (3A) is taken:

$$\rho sU(r,s)=-\frac{2\mu U(r,s)}{r^2}+\mu\frac{d^2U(r,s)}{dr^2}+2\mu\frac{1}{r}\frac{dU(r,s)}{dr} \tag{6A}$$

The general solution of Eq. (6A) is

$$U(r,s)=-\frac{1}{r^2}\left[c_1(-\sqrt{\mu}+r\sqrt{\rho s})e^{r\sqrt{\frac{\rho s}{\mu}}}+c_2(\sqrt{\mu}+r\sqrt{\rho s})e^{-r\sqrt{\frac{\rho s}{\mu}}}\right] \tag{7A}$$

We first apply a third-order Taylor series expansion of the function (7A) about $r=0$ to avoid singularity at the center of the sphere:

$$U(r,s)=\frac{1}{2\sqrt{\mu}}\left(\frac{2\mu c_1-2\mu c_2}{r^2}-c_1\rho s+c_2\rho s\right) \tag{8A}$$

where $c_1=c_2$ for the velocity to be defined at the origin. Eq. (7A) becomes

$$U(r,s)=-\frac{c_1}{r^2}\left[(-\sqrt{\mu}+r\sqrt{\rho s})e^{r\sqrt{\frac{\rho s}{\mu}}}+(\sqrt{\mu}+r\sqrt{\rho s})e^{-r\sqrt{\frac{\rho s}{\mu}}}\right] \tag{9A}$$

with the transformed boundary condition:

$$U(R,s)=\frac{V}{s} \tag{10A}$$

After applying Eq. (10A), Eq. (9A) is written as

$$U(r,s)=\frac{VR^2\left(-\sqrt{\mu}e^{r\sqrt{\frac{\rho s}{\mu}}}+r\sqrt{\rho s}e^{r\sqrt{\frac{\rho s}{\mu}}}+r\sqrt{\rho s}e^{-r\sqrt{\frac{\rho s}{\mu}}}+\sqrt{\mu}e^{-r\sqrt{\frac{\rho s}{\mu}}}\right)}{sr^2\left(-\sqrt{\mu}e^{R\sqrt{\frac{\rho s}{\mu}}}+R\sqrt{\rho s}e^{R\sqrt{\frac{\rho s}{\mu}}}+R\sqrt{\rho s}e^{-R\sqrt{\frac{\rho s}{\mu}}}+\sqrt{\mu}e^{-R\sqrt{\frac{\rho s}{\mu}}}\right)} \tag{11A}$$

The steady-state velocity is

$$\lim_{t\to\infty}[u(r,t)]=\lim_{s\to 0}[sU(r,s)]=\frac{Vr}{R} \tag{12A}$$

The residue theorem is used to determine $u(r,t)$ in the form:

$$u(r,t)=\frac{Vr}{R}+\sum_{n=1}^{\infty}\frac{P_1(r,s_n)}{\frac{dQ_1(s)}{ds}\Big|_{s=s_n}}e^{s_n t} \tag{13A}$$

where $P_1(r,s)$ and $Q_1(s)$ are the numerator and denominator of Eq. (11A). The poles s_n are obtained by setting $Q_1(s)=0$:

$$-\sqrt{\mu}e^{R\sqrt{\frac{\rho s}{\mu}}}+R\sqrt{\rho s}e^{R\sqrt{\frac{\rho s}{\mu}}}+R\sqrt{\rho s}e^{-R\sqrt{\frac{\rho s}{\mu}}}+\sqrt{\mu}e^{-R\sqrt{\frac{\rho s}{\mu}}}=0 \tag{14A}$$

After writing the poles in terms of a positive constant α_n^2:

$$s_n=-\frac{\alpha_n^2\mu}{\rho R^2} \tag{15A}$$

Eq. (14A) becomes

$$-2\sqrt{\mu}\sin(\alpha_n)+2\alpha_n\sqrt{\mu}\cos(\alpha_n)=0 \tag{16A}$$

or

$$\tan(\alpha_n)=\alpha_n \tag{17A}$$

Finally, the velocity is

$$u(r,t)=\frac{Vr}{R}+\sum_{n=1}^{\infty}\frac{2VR\left[R\sin\left(\frac{\alpha_n r}{R}\right)-\alpha_n r\cos\left(\frac{\alpha_n r}{R}\right)\right]}{r^2\alpha_n^2\sin(\alpha_n)}e^{-\frac{\alpha_n^2\mu}{\rho R^2}t} \tag{18A}$$

For large μ, the summation in Eq. (18A) approaches 0 very fast and the velocity is simplified to

$$u(r,t)=\frac{Vr}{R} \tag{19A}$$

or

$$\frac{\partial u(r,t)}{\partial r}=\frac{V}{R}=\frac{1}{R}\frac{dR}{dt} \tag{20A}$$

Eq. (20A) is also valid if for time-dependent density fluid assuming that ρ changes slowly ($d\rho/dt\approx 0$). For such systems, it can be shown that Eq. (18A) becomes

$$u(r,t)=\frac{Vr}{R}+\sum_{n=1}^{\infty}\frac{2VR\left[R\sin\left(\frac{\alpha_n r}{R}\right)-\alpha_n r\cos\left(\frac{\alpha_n r}{R}\right)\right]}{r^2\alpha_n^2\sin(\alpha_n)}e^{-\frac{\alpha_n^2\mu}{\rho R^2}\int_0^t\rho(\sigma)d\sigma} \tag{21A}$$

Similarly, the summation in Eq. (21A) converges to 0 quickly for large μ and the expression for the velocity is simplified to Eq. (19A) given that

$$\int_0^t\frac{1}{\rho(\sigma)}d\sigma>0 \tag{22A}$$

References

Bierbrauer, F., 2005. Hydrogel Drug Delivery: Diffusion Models, Internal Report. School of Mathematics & Applied Statistics, University of Wollongong.

Bradford, M.M., 1976. A rapid and sensitive method for the quantitation of microgram quantities of protein utilizing the principle of protein-dye binding. Anal. Biochem. 2 (1–2), 248–254.

Brazel, C.S., Peppas, N.A., 1999. Dimensionless analysis of swelling of hydrophilic glassy polymers with subsequent drug release from relaxing structures. Biomaterials 20 (8), 721–732.

Chen, J., Blevins, W.E., Park, H., Park, K., 2000. Gastric retention properties of superporous hydrogel composites. J Control Release 64 (1–3), 39–51.

Chivukula, P., Dusek, K., Wang, D., Duskova-Smrckova, M., Kopeckova, P., Kopecek, J., 2006. Synthesis and characterization of novel aromatic azo bond-containing pH-sensitive and hydrolytically cleavable IPN hydrogels. Biomaterials 27 (7), 1140–1151.

Collins, R., 1980. The choice of an effective time constant for diffusive processes in finite systems (thermal conduction and sputtering examples). J. Phys. D Appl. Phys. 13 (11), 1935.

Gupta, P., Vermani, K., Garg, S., 2002. Hydrogels: from controlled release to pH-responsive drug delivery. Drug Discov Today 7 (10), 569–579.

Klumb, L.A., Horbett, T.A., 1992. Design of insulin delivery devices based on glucose sensitive membranes. J. Controlled Release 18 (1), 59–80.

Kost, J., Horbett, T.A., Ratner, B.D., Singh, M., 1985. Glucose-sensitive membranes containing glucose oxidase: activity, swelling, and permeability studies. J. Biomed. Mater. Res. 19 (9), 1117–1133.

Mahmoud, E.A., Bendas, E.R., Mohamed, M.I., 2010. Effect of formulation parameters on the preparation of superporous hydrogel self-nanoemulsifying drug delivery system (SNEDDS) of carvedilol. AAPS PharmSciTech 11 (1), 221–225.

Martinez-Ruvalcaba, A., Sanchez-Diaz, J., Becerra, F., Cruz-Barba, L., Gonzalez-Alvarez, A., 2009. Swelling characterization and drug delivery kinetics of polyacrylamide-co-itaconic acid/chitosan hydrogels. Express Polym. Lett. 3 (1), 25–32.

Mitchell, M., 2007. Engauge Digitizer – Version 4.1.

Naddaf, A.A., Tsibranska, I., Bart, H.J., 2010. Kinetics of BSA release from poly(N-isopropylacrylamide) hydrogels. Chem. Eng. Process. 49 (6), 581–588.

Neeraj, A., Chandrasekar, M.J., Sara, U.V., Rohini, A., 2011. Poly(HEMA-Zidovudine) conjugate: a macromolecular pro-drug for improvement in the biopharmaceutical properties of the drug. Drug Deliv. 18 (4), 272–280.

Panyam, J., Labhasetwar, V., 2003. Biodegradable nanoparticles for drug and gene delivery to cells and tissue. Adv. Drug Deliv. Rev. 55 (3), 329–347.

Patel Vijay, R., Amiji Mansoor, M., 1996. pH-sensitive swelling and drug-release properties of chitosan-poly(ethylene oxide) semi-interpenetrating polymer network. In: Hydrogels and Biodegradable Polymers for Bioapplications, American Chemical Society, vol. 627, pp. 209–220.

Pirvu, C., 2004. Evaluation of gelatin microspheres with xantinol nicotinate. Rom. J. Biophys. 14, 81–88.

Qiu, Y., Park, K., 2001. Environment-sensitive hydrogels for drug delivery. Adv. Drug Deliv. Rev. 53 (3), 321–339.

Rasmussen, M.R., Snabe, T., Pedersen, L.H., 2003. Numerical modelling of insulin and amyloglucosidase release from swelling Ca-alginate beads. J. Control. Release 91 (3), 395–405.

Schott, H., 1992. Kinetics of swelling of polymers and their gels. J. Pharm. Sci. 81 (5), 467–470.

Shavi, G.V., Nayak, U.Y., Reddy, M.S., Karthik, A., Deshpande, P.B., Kumar, A.R., Udupa, N., 2011. Sustained release optimized formulation of anastrozole-loaded chitosan microspheres: in vitro and in vivo evaluation. J. Mater. Sci. Mater. Med. 22 (4), 865–878.

Simon, L., 2013. Control of Biological and Drug-Delivery Systems for Chemical, Biomedical, and Pharmaceutical Engineering. Wiley, Hoboken, N.J., p. xv, 366p.

Sivanantham, M., Tata, B.V.R., 2012. Swelling/deswelling of polyacrylamide gels in aqueous NaCl solution: light scattering and macroscopic swelling study. Pramana 79 (3), 457–469.

Tanaka, T., 1979. Phase transitions in gels and a single polymer. Polymer 20 (11), 1404–1412.

Torres-Lugo, M., Peppas, N.A., 1999. Molecular design and in vitro studies of novel pH-sensitive hydrogels for the oral delivery of calcitonin. Macromolecules 32 (20), 6646–6651.

Zrinyi, M., Rosta, J., Horkay, F., 1993. Studies on the swelling and shrinking kinetics of chemically crosslinked disk-shaped poly(vinyl acetate) gels. Macromolecules 26 (12), 3097–3102.